Boundary Layer Length Scales in Thermal Turbulence

Andrew Belmonte, Andreas Tilgner, and Albert Libchaber[(a)]
Physics Department, Princeton University, Princeton, New Jersey 08544
(Received 29 March 1993)

We present measurements of local temperature fluctuations from a convection cell of aspect ratio 1, using gas at room temperature, for Rayleigh numbers (Ra) ranging from 5×10^5 to 1×10^{11}. The thermal boundary layer thickness is measured; its scaling is close to $\mathrm{Ra}^{-2/7}$ for $\mathrm{Ra}>2\times10^7$. A second length scale is measured through the cutoff frequency of the power spectrum, which we relate to the velocity of the large scale circulation. The Rayleigh number dependence of this length changes at $\mathrm{Ra}=2\times10^9$.

PACS numbers: 47.27.Nz, 47.27.Te

The study of Rayleigh-Bénard convection has led to the experimental determination of different turbulent states at high Rayleigh numbers [1–3]. These states are characterized through statistical quantities such as the average heat flux, mean circulation velocity, and local temperature fluctuations. In the highest Rayleigh number state, called hard turbulence, the measured quantities have a power law dependence on Rayleigh number. Turbulent convection involves temperature and velocity fields which have boundary layers at the limiting surfaces. Direct characterization of these boundary layers had been neglected until a recent experiment with water at a Rayleigh number of about 10^9 [4].

In this Letter we present results from an aspect ratio 1 cell using room temperature gas, with a Prandtl number of 0.7, and Rayleigh numbers ranging from 5×10^5 to 1×10^{11}. By recording local temperature fluctuations at varying distances from the colder plate, we measure the thermal boundary layer thickness. We also measure a second length scale using the high frequency cutoff of the power spectra, and argue that this length scale is related to the velocity field.

The experimental conditions are simply described: Planar boundaries, above and below the flow region, maintain a constant temperature difference across the fluid, which is also confined by lateral, thermally insulating boundaries. The situation is completely specified by three dimensionless parameters [5]: The Rayleigh and Prandtl numbers, and the aspect ratio of the cell, which quantifies its geometry. The Rayleigh number is defined as

$$\mathrm{Ra}=g\alpha\Delta L^3/\nu\kappa,$$

where g is the gravitational acceleration, L the height of the cell, Δ the temperature difference, α the thermal expansion coefficient of the fluid, ν its kinematic viscosity, and κ its thermal diffusivity. The Prandtl number is the ratio of the two diffusion constants: $\mathrm{Pr}=\nu/\kappa$. The aspect ratio is the lateral extent of the cell divided by the height L.

A detailed description of our apparatus will be published elsewhere [6]. The convection cell is a cube 15.2 cm in height, contained within a larger steel vessel designed to withstand pressures of up to 50 atm [7]; both are filled with gas at room temperature, and a small hole in the cell allows the pressure in the vessel and cell to equilibrate. The vessel is also filled with cotton batting so as to impede the movement of gas exterior to the cell. By varying the pressure from 0.6 to 18 atm, and filling the cell with helium, nitrogen, or sulfur hexafluoride (SF_6), we could span almost six decades of Rayleigh number, while the Prandtl number remained constant to within 5%. The temperature fluctuations were measured below the center of the colder (top) plate with an uncoated metal oxide thermistor about 200 μm in diameter [8]. A microtranslational stage was used to vary the height of the detector, and several thermistors were used to cover the upper half of the cell along its center axis [5].

The experiment was designed to visualize turbulent convection [6]. Using shadowgraph techniques, we have observed a single circulating roll in the cell for Ra up to 10^{10}, and estimated advection velocities to be around 10 cm/s.

We first present the thermal boundary layer measure-

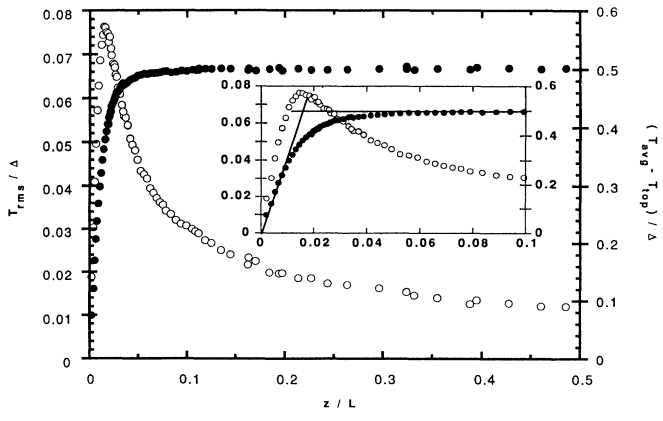

FIG. 1. The normalized mean (black dots) and rms (open dots) temperature profiles vs z/L, for SF_6 at $\mathrm{Ra}=4.8\times10^7$ and $\Delta=16.3\,^\circ\mathrm{C}$; $L=15.2$ cm. The mean is plotted as $(T-T_{\mathrm{top}})/\Delta$, so that the top plate temperature is zero, and the central temperature is 0.5. The inset shows an enlargement of the region close to the plate.

0031-9007/93/70(26)/4067(4)$06.00

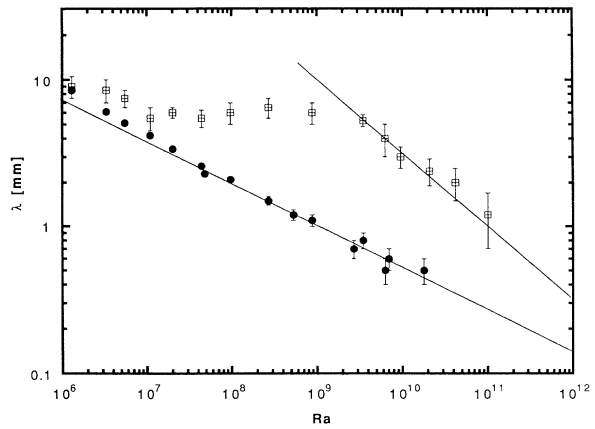

FIG. 2. The length scales λ_{th} (circles) and λ_m (squares) vs Ra, with error bars of ± 0.1 and ± 1 mm, respectively. The line drawn for λ_{th} corresponds to $\mathrm{Ra}^{-0.29}$; the line for λ_m corresponds to $\mathrm{Ra}^{-1/2}$.

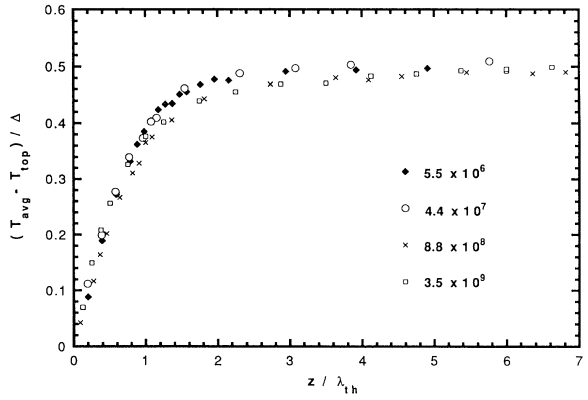

FIG. 3. The normalized mean temperature profiles vs z/λ_{th} for several Ra. The distance z is normalized by the thermal boundary layer thickness.

ments. Figure 1 shows a typical profile of the mean and root-mean-squared (rms) values of the temperature as a function of the distance z from the top plate (normalized by the cell height L) for $\mathrm{Ra}=4.8\times10^7$. Half of the total temperature difference Δ occurs in a layer close to the top plate, in which the z dependence of the mean temperature is at first linear. We define the thermal boundary layer thickness as the distance λ_{th} at which the extrapolation of the linear portion of the profile equals the central mean temperature [5]. The temperature rms reaches a maximum at approximately this same position, and then decreases as one moves into the cell [4]. The measured thickness λ_{th} is plotted against Ra in Fig. 2.

For $\mathrm{Ra}>2\times10^7$, we find that $\lambda_{th}\sim\mathrm{Ra}^{-0.29\pm0.01}$. From this, we estimate the local Nusselt number [9] as

$$\mathrm{Nu}=L/2\lambda_{th}=0.18\,\mathrm{Ra}^{0.29\pm0.01}.$$

In similar experiments on low temperature helium gas, direct measurement of the heat flux led to $\mathrm{Nu}=0.22\mathrm{Ra}^{0.285\pm0.004}$ for $\mathrm{Ra}>4\times10^7$ [2,3]. Those experiments also found that below 4×10^7, the Nusselt number is closer to $\mathrm{Ra}^{1/3}$; we note an increase in the slope for $\mathrm{Ra}<2\times10^7$ in Fig. 2.

Figure 3 shows the mean temperature profile for several different Ra, normalized by the thermal boundary layer thickness. There is clearly no universal shape, but perhaps two characteristic ones, indicating a possible transition somewhere above 10^8. This observation will be addressed later in the paper.

We now move to the velocity boundary layer. We have not found a viable method for directly measuring velocity in our experiment [10]. We were, however, guided by an observation from our experiment with water, in which the velocity layer was measured directly [4]. By looking at the changes in the power spectrum of local temperature fluctuations with height, a correspondence was found between the high frequency cutoff of the spectrum and the velocity profile. In the present experiment we also examine the power spectra as a function of height, and find that the high frequency cutoff varies with z. A typical time series and its spectrum [11] are shown in Fig. 4. For experimental convenience, we define *the cutoff frequency* f_c as the frequency where the power spectrum intersects the noise level of the experiment. The signal-to-noise ratio was approximately constant during measurements, and small variations did not significantly affect the measured value of f_c.

A typical profile of f_c normalized by the characteristic frequency κ/L^2 is shown in Fig. 5 for $\mathrm{Ra}=8.8\times10^8$. The inset shows a linear region of f_c close to the plate, which extrapolates to a nonzero value of f_c at $z=0$. Further into the cell, f_c reaches a maximum. The position of this maximum, λ_m, is plotted against Ra in Fig. 2.

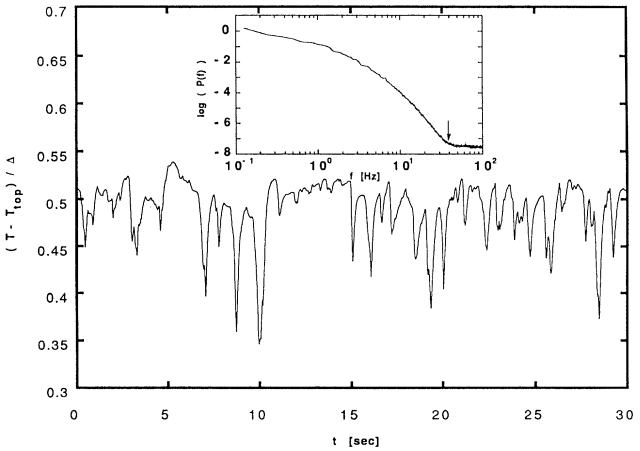

FIG. 4. A typical time series of temperature fluctuations at $z=4$ mm, for SF_6 at $\mathrm{Ra}=8.8\times10^8$ and $\Delta=21.7\,^\circ$C. The inset shows the power spectrum taken over 30 min. The arrow indicates the cutoff frequency ($f_c\sim40$ Hz).

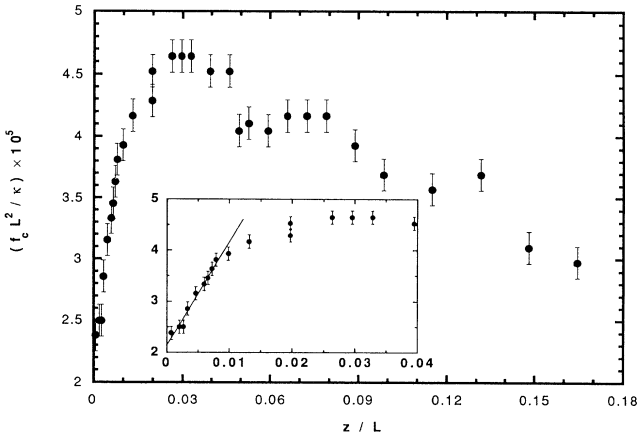

FIG. 5. The cutoff frequency for SF_6 at $Ra = 8.8\times10^8$ and $\Delta = 21.7\,^\circ C$. The inset shows the region close to the plate.

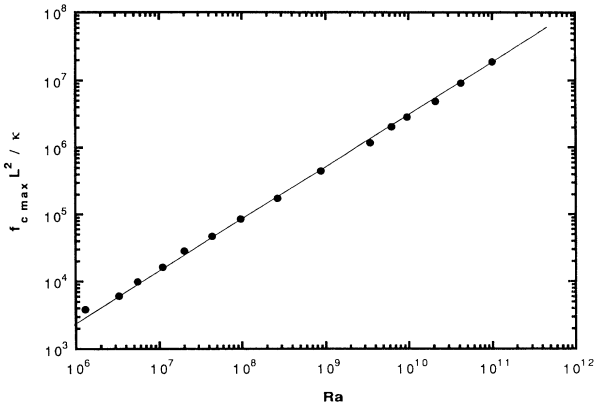

FIG. 6. A plot of $f_{c\max}L^2/\kappa$ vs Ra. The line corresponds to $Ra^{0.79}$.

The value of the maximum cutoff frequency ($f_{c\max}$) has a well defined scaling with Ra. Figure 6 shows the dimensionless value of $f_{c\max}$ at each Ra. They scale as $Ra^{0.79\pm0.03}$ from $Ra = 4\times10^6$ to the highest Rayleigh number attained in our experiment (1×10^{11}).

We now propose an interpretation for the maximum in the cutoff frequency. The higher frequencies of the power spectrum have their origin in the narrower peaks of the time series. Temperature fluctuations close to the top plate include many sharp excursions to lower temperatures (as in Fig. 4) due to boundary layer detachments being advected past the detector. The temporal width of these peaks is determined by both the spatial width of the detachments (Λ) and their advection speed (u). The cutoff frequency, as a measure of the high frequency extent of the spectrum, is then $f_c \sim u/\Lambda$. The typical length scale for detachments in the region near the boundary layer is roughly the boundary layer thickness λ_{th}, independent of height [12] (all measurements presented here are in the region $z/L < 0.16$). Therefore u and f_c must be maximum at the same point. We know from visualization that the large scale circulation supplies the dominant velocity (U) in the region close to the plate, so that $f_c \sim U/\lambda_{th}$. We can use the scaling for the circulation velocity measured previously [3], neglecting small variations of velocity with distance (because the maximum of f_c is broad), to write

$$\frac{f_{c\max}L^2}{\kappa} \sim \frac{Ra^{1/2}}{Ra^{-2/7}} \sim Ra^{11/14};$$

$11/14 = 0.786$ is close to the observed exponent 0.79. This agreement lends strong support to the identification of the position of the maximum velocity with the position of the maximum cutoff frequency.

It is surprising then that the measured scaling for the maximum f_c extends below $Ra = 2\times10^7$ (Fig. 6), since the behavior of λ_{th} is different in this regime. However, a change in the behavior of the large scale circulation has also been observed for $Ra < 4\times10^7$ [2]. The velocity is larger than would be expected from $U \sim Ra^{1/2}$, which would tend to compensate for the change in λ_{th}. Thus a change in the scaling could be unnoticeable.

In light of our interpretation we now discuss the dependence of λ_m on Rayleigh number. Its most striking feature is the gap that opens between the two length scales above $Ra \sim 10^7$ (Fig. 2), which we divide into two different regimes. The first regime is characterized by the observation that $\lambda_m \sim$ const (at about 6 mm). We have no explanation as to why this occurs. We only note that it allows the Reynolds number of the velocity layer to increase: At $Ra = 2\times10^7$, we estimate the Reynolds number to be about 50, whereas at $Ra = 2\times10^9$, it is about 600 [13]. Thus the velocity boundary layer is not yet turbulent (in the Reynolds number sense) at the transition to hard turbulence [14].

In the second regime, for $Ra > 2\times10^9$, λ_m decreases as $Ra^{-0.44\pm0.09}$. If we approximate this exponent by -0.5, we find that the Reynolds number of the velocity layer remains at about 600. Reynolds numbers on the order of 10^3 are reasonable for a turbulent layer. Thus above $Ra \sim 10^9$ the velocity layer is governed primarily by inertia.

The transition at $Ra = 2\times10^9$ does not affect the scaling of λ_{th}; nor was an effect seen in the measurements of previous experiments [2,3]. This may be because λ_{th} is well within the velocity layer at $Ra \sim 10^9$. The shape of the mean temperature profile does appear to change, however, as seen in Fig. 3. The rounded portion of the profile, outside the boundary layer, becomes more gradual for $Ra > 10^9$, which may indicate a broadened mixing zone. Note that because the linear portion of the profiles coincide, the Nusselt number is unaffected.

The scaling of the velocity layer, if extrapolated, suggests that the hard turbulence state is not asymptotic, since thermal and viscous layers might cross at a much higher Rayleigh number. This has also been suggested in a recent model [15]. Hard turbulence would then be an

intermediate state, owing its existence to the gap between the boundary layer length scales of the temperature and velocity. It appears that the deeper one looks into turbulence, the more complexity and substructure emerge.

This work was supported under NSF Grant No. DMR 8722714. A.T. gratefully acknowledges the support of a NATO grant from the "Deutscher Akademischer Austauschdienst."

---

[a]Also at NEC Research Institute, 4 Independence Way, Princeton, NJ 08540.

[1] W. V. R. Malkus, Proc. R. Soc. London A **225**, 185 (1954); D. B. Thomas and A. A. Townsend, J. Fluid Mech. **2**, 473 (1957); G. E. Willis and J. W. Deardorff, Phys. Fluids **10**, 1861 (1967); T. Y. Chu and R. J. Goldstein, J. Fluid Mech. **60**, 141 (1973); D. C. Threlfall, J. Fluid Mech. **67**, 17 (1975); R. Krishnamurti and L. N. Howard, Proc. Natl. Acad. Sci. U.S.A. **78**, 1981 (1981).

[2] M. Sano, X. Z. Wu, and A. Libchaber, Phys. Rev. A **40**, 6421 (1989).

[3] X. Z. Wu, Ph.D. thesis, University of Chicago, 1991 (unpublished).

[4] A. Tilgner, A. Belmonte, and A. Libchaber, Phys. Rev. E **47**, 2253 (1993).

[5] In the Boussinesq approximation of the Navier-Stokes and heat equations, density variations are retained only for the buoyancy term; all other fluid properties are assumed to be temperature independent. There is then a symmetry between the top and bottom halves of the cell, and the central temperature is $T_{\text{top}}+\Delta/2$.

[6] A. Belmonte, A. Tilgner, and A. Libchaber (to be published).

[7] Designed by E. Moses.

[8] Type BB05, obtained from Thermometrics Inc., 808 U.S. Highway 1, Edison, NJ 08817.

[9] The Nusselt number is the heat flux normalized by its value for pure conduction. By assuming that the heat is transported by diffusion across the two boundary layers, and by turbulent advection across the rest of the cell (a negligible thermal resistance by comparison), one gets $\text{Nu}=L/2\lambda_{\text{th}}$.

[10] A previous technique for measuring mean advection velocities in gas (Ref. [3]) is impractical for our experiment due to the proximity of the detectors to the fluctuating boundary layer. Instead, we modify the method of comparing the signals from two detectors of known separation, by measuring the delay time for only those fluctuations which are recognizably similar. Although this is a cumbersome procedure, we have estimated velocities of 8.5 and 8.0 cm/s at λ_m, for $\text{Ra}=1.3\times10^9$ and 9.7×10^9, respectively. These velocities agree well with those measured previously in Ref. [3].

[11] The shape of the power spectrum in turbulent convection has been studied in previous works. See X. Z. Wu, L. Kadanoff, A. Libchaber, and M. Sano, Phys. Rev. Lett. **64**, 2140 (1990), and references therein.

[12] G. Zocchi, E. Moses, and A. Libchaber, Physica (Amsterdam) **166A**, 387 (1990).

[13] To estimate the Reynolds number at λ_m, we extrapolate the velocity measurements in Ref. [10], using $U\sim\text{Ra}^{1/2}$.

[14] Although the Reynolds number based on the height of the cell is about 1000 at $\text{Ra}=2\times10^7$. The same values for these Reynolds numbers were measured in water at $\text{Ra}=1.1\times10^9$ (in Ref. [4]).

[15] B. I. Shraiman and E. D. Siggia, Phys. Rev. A **42**, 3650 (1990).